Action Potential Morphology Influences Intracellular Calcium Handling Stability and the Occurrence of Alternans

Peter N. Jordan* and David J. Christini*†

*Department of Physiology and Biophysics, Weill Graduate School of Medical Sciences of Cornell University, New York, New York, 10021; and †Division of Cardiology, Department of Medicine, Weill Medical College of Cornell University, New York, New York, 10021

ABSTRACT Instability in the intracellular Ca^{2+} handling system leading to Ca^{2+} alternans is hypothesized to be an underlying cause of electrical alternans. The highly coupled nature of membrane voltage and Ca^{2+} regulation suggests that there should be reciprocal effects of membrane voltage on the stability of the Ca^{2+} handling system. We investigated such effects using a mathematical model of the cardiac intracellular Ca^{2+} handling system. We found that the morphology of the action potential has a significant effect on the stability of the Ca^{2+} handling system at any given pacing rate, with small changes in action potential morphology resulting in a transition from stable nonalternating Ca^{2+} transients to stable alternating Ca^{2+} transients. This bifurcation occurs as the alternans eigenvalue of the system changes from absolute value <1 to absolute value >1. These results suggest that the stability of the intracellular Ca^{2+} handling system and the occurrence of Ca^{2+} alternans are not dictated solely by the Ca^{2+} handling system itself, but are also modulated to a significant degree by membrane voltage (through its influence on sarcolemmal Ca^{2+} currents) and, therefore, by all ionic currents that affect membrane voltage.

INTRODUCTION

Cardiac electrical alternans appears to be a diagnostic indicator for vulnerability to arrhythmias (1–4). Recent evidence also demonstrates that electrical alternans can provide a suitable substrate for the initiation of reentry, suggesting a potential mechanistic link to the onset of arrhythmias (5–8). Recent research has focused on understanding the physiological mechanisms underlying alternans (9–19), and on developing new ways of eliminating alternans (15,20–25).

Particular interest has been paid to the role of the intracellular Ca^{2+} handling system in electrical alternans (26). This focus is due in part to experiments conducted in isolated rabbit ventricular myocytes, where it was demonstrated that the intracellular Ca^{2+} transient could alternate on a beat-to-beat basis during voltage clamping even though the applied voltage waveform was a train of identical action potentials (27). This demonstration, that Ca^{2+} alternans may occur independently of electrical alternans, appears to support the hypothesis that electrical alternans is caused by Ca^{2+} alternans (26). Based on this hypothesis, mathematical modeling has suggested that the intracellular Ca^{2+} handling system instability that leads to Ca^{2+} alternans during voltage clamping (i.e., in the absence of electrical alternans) can be explained by a steep and nonlinear dependence of Ca^{2+} release from the sarcoplasmic reticulum (SR) on SR Ca^{2+} load and diastolic Ca^{2+} concentration (19,28,29). Recent experimental results also point to the importance of the steep dependence of Ca^{2+} release on SR Ca^{2+} load and diastolic Ca^{2+} concentration (13,30).

Although the properties of the SR are important in understanding the regulation of intracellular Ca^{2+} concentration, other processes such as the passage of Ca^{2+} through voltage- and Ca^{2+}-sensitive L-type Ca^{2+} channels (I_{Ca}) and Na^{+}-Ca^{2+} exchangers (I_{NaCa}) also play a role in Ca^{2+} regulation. The voltage-sensitive gating of these sarcolemmal currents suggests that the morphology of the action potential should influence their activity and, therefore, the occurrence of Ca^{2+} alternans. Action potential clamp experiments conducted using rat and rabbit ventricular myocytes have shown that the morphology of the voltage waveform does have a marked influence on the shape of the intracellular Ca^{2+} transient (31). However, these experiments were conducted at excitation rates that were too slow for Ca^{2+} alternans to develop. In a mathematical model of intracellular Ca^{2+} handling that reproduces the rabbit ventricular myocyte action potential clamp experiments discussed above (29), and in recent experiments investigating Ca^{2+} alternans in rat myocytes during voltage clamping (13), it was demonstrated that the Ca^{2+}-selective sarcolemmal currents alternate during Ca^{2+} alternans. These currents alternated despite being clamped by voltage waveforms that were identical on a beat-to-beat basis. However, the influence of different voltage waveforms on the behavior of the intracellular Ca^{2+} handling system and the incidence of Ca^{2+} alternans was not investigated in these studies. Recent experiments with epicardial and endocardial myocytes isolated from guinea pig hearts investigated the onset of Ca^{2+} alternans in response to two different action potential morphologies during action potential clamping (30). This study found that the excitation rate at which Ca^{2+} alternans was initiated during clamping did not depend upon which of the two action potentials were used to perform clamping (Figs. 2 and 4 in Wan et al. (30)). However, the influence of action potential morphology on Ca^{2+} handling

Submitted July 22, 2005, and accepted for publication September 28, 2005.

Address reprint requests to David J. Christini, PhD, Div. of Cardiology, Weill Medical College of Cornell University, 520 East 70th St., Starr 463, New York, NY 10021. Tel.: 212-746-6280; Fax: 212-746-8451; E-mail: dchristi@med.cornell.edu.

0006-3495/06/01/672/09 $2.00

doi: 10.1529/biophysj.105.071340

system stability was not systematically investigated in these experiments.

The influence of action potential morphology at any given excitation rate on the stability of the Ca^{2+} handling system and the development of Ca^{2+} alternans therefore remains poorly understood. Using the mathematical model that reproduces the action potential clamp experiments discussed above (29), we explored the stability of the Ca^{2+}-handling system in response to different action potential morphologies. We demonstrate that the morphology of the action potential during voltage clamping is a significant factor in determining the stability of the Ca^{2+}-handling system, and therefore plays an important role in determining whether Ca^{2+} alternans occurs. Given that the morphology of the action potential waveform during voltage clamping reflects the contribution of every membrane current, this suggests that every membrane current, and not just those of the Ca^{2+} handling system, influences the conditions under which alternans occurs.

MATERIALS AND METHODS

Mathematical model

Simulations were performed using a model of the intracellular Ca^{2+} handling system of a ventricular myocyte subjected to action potential voltage clamping (29). The model incorporates cytosolic, submembrane, junctional SR, and network SR Ca^{2+} concentrations, L-type Ca^{2+} (I_{Ca}), Na^+-Ca^{2+} exchange (I_{NaCa}), and SR uptake (I_{up}) currents, Ca^{2+}-induced Ca^{2+} release from the SR, and Ca^{2+} buffering. The membrane voltage was clamped according to

$$V(t) = \begin{cases} V_{\min} + (V_{\max} - V_{\min})\sqrt{1 - \left(\frac{t-mT}{xT}\right)^{\beta}} & mT \le t \le (m+x)T \\ V_{\min} & (m+x)T < t < (m+1)T, \end{cases} \quad (1)$$

where $V_{\min} = -80\,\text{mV}$, $V_{\max} = 30\,\text{mV}$, T is the pacing period (in seconds), m denotes beat number, and β and x are parameters that characterize the morphology of the action potential. The parameter β allows the shape of the action potential in the plateau and repolarization phases to be varied while changing the action potential duration at 90% repolarization only slightly (if at all). β was varied between 0.8 and 2.0 in our simulations ($\beta = 2.0$ was the value used in the original modeling study (29)). The parameter x, which is the ratio of action potential duration to pacing period, varies with T according to

$$x(T) = \frac{0.67}{0.67 + T}. \quad (2)$$

Stability analysis

The stability of the intracellular Ca^{2+} handling system was characterized using the ''eigenmode'' method (10), which was adapted to analyze the intracellular Ca^{2+}-handling model used in this study. Briefly, the method involves: i), locating the period-1 (i.e., no alternans) solution for a given pacing period T (which may be inherently stable, as in situations where no Ca^{2+} alternans naturally occurs at that value of T, or inherently unstable, as in situations where Ca^{2+} alternans naturally occurs at that value of T); ii), systematically applying small perturbations to each state variable (i.e., Ca^{2+} concentrations, ion channel gating variables, etc.); and iii), calculating the eigenvalues of the system from the response of the state variables to the perturbations. As there are nine state variables in the model (V, $[Ca^{2+}]_s$, $[Ca^{2+}]_i$, $[Ca^{2+}]_j$, $[Ca^{2+}]_j'$, I_{rel}, f, q, $[CaT]_i$, and $[CaT]_s$; see Shiferaw et al. (29) for details), nine eigenvalues are calculated for each set of conditions. The alternans eigenvalue (λ_a), defined as the largest negative eigenvalue (10), characterizes the stability of the corresponding alternans eigenmode, and hence characterizes the stability of the period-1, nonalternating rhythm. If $|\lambda_a| < 1$, a stable, period-1, nonalternating rhythm will be present, whereas if $|\lambda_a| > 1$, the period-1 rhythm is unstable. Systems characterized by larger values of $|\lambda_a|$ are less stable than systems characterized by smaller values of $|\lambda_a|$.

RESULTS

Fig. 1 illustrates the effect of changing the value of β in Eq. 1 on the morphology of the action potential waveform applied during voltage clamping at a pacing period $T = 300$ ms. As Fig. 1 *A* illustrates, varying β markedly changes the slope of the plateau phase of the action potential (as indicated by the different action potential duration (APD) restitution curves calculated at 50% repolarization). Over this range of β-values the APD at 90% repolarization is practically identical (as indicated by the overlapping APD restitution curves at 90% repolarization).

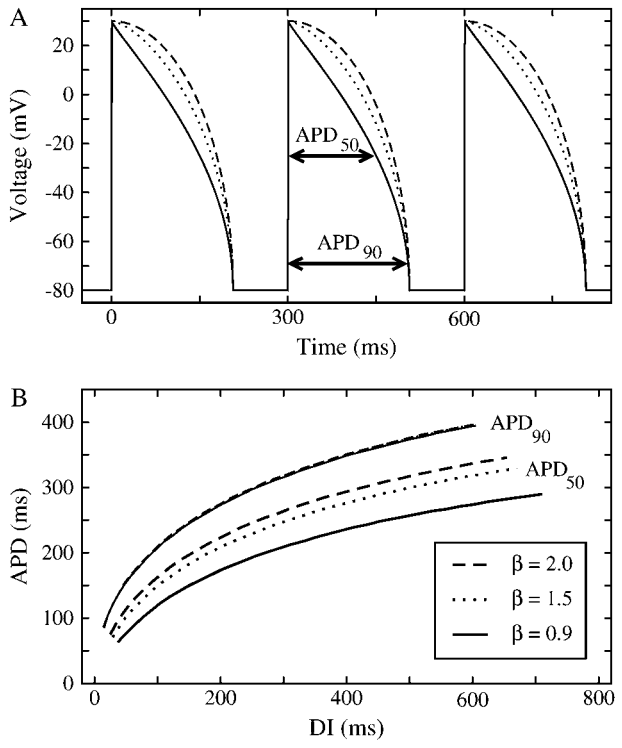

FIGURE 1 (*A*) Action potential morphology as a function of the parameter β (see Eq. 1) at a pacing period of $T = 300$ ms. (*B*) Action potential duration (*APD*) restitution curves for the three values of β in panel *A*, measured at both 50% (APD_{50}) and 90% (APD_{90}) repolarization. As panel *B* indicates, APD and diastolic interval (*DI*) measured at 90% repolarization are practically identical for the values of β shown.

Action potential morphology and Ca^{2+} alternans

Fig. 2 shows how changing the morphology of the action potential waveform at a given excitation rate influences the occurrence of Ca^{2+} alternans. As Fig. 2 *A* indicates, $\beta = 2.0$ at a pacing period $T = 300$ ms results in stable, period-2 Ca^{2+} alternans, whereas $\beta = 0.9$ at the same pacing period results in stable, period-1, nonalternating behavior. Fig. 2 also illustrates the activity of the Ca^{2+} currents I_{NaCa} (Fig. 2 *B*) and I_{Ca} (Fig. 2 *C*), with both currents alternating for $\beta = 2.0$ but neither current alternating for $\beta = 0.9$. Given that the intrinsic properties of the system (e.g., ionic current conductances, pump, and exchanger strengths) and the pacing period are identical for both values of β, Fig. 2 suggests that, at any given pacing period, the voltage waveform sensed by the sarcolemmal Ca^{2+} channels and exchangers (and not just the APD, diastolic interval (DI), or pacing period) is intimately involved in determining whether the intracellular Ca^{2+} handling system generates nonalternating or alternating Ca^{2+} transients.

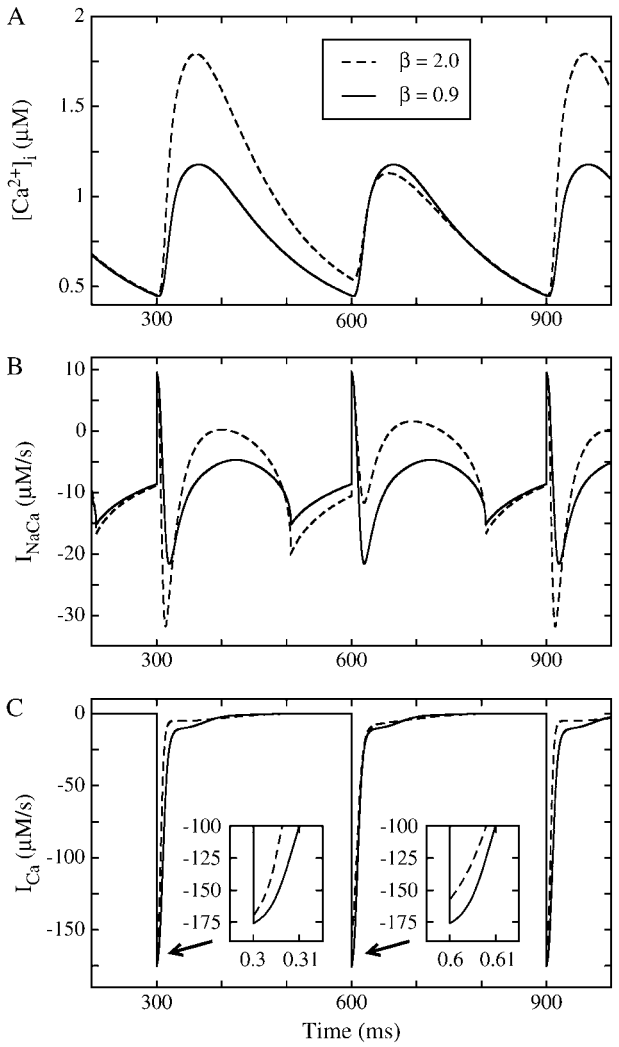

FIGURE 2 (*A*) Intracellular Ca^{2+} concentration, (*B*) Na^{+}-Ca^{2+} exchange current, and (*C*) L-type Ca^{2+} channel current for two different values of β at a pacing period of $T = 300$ ms. When $\beta = 2.0$, all three components exhibit a stable period-2 alternans rhythm. For $\beta = 0.9$ alternans does not occur in any component, indicating that the period-1, nonalternating rhythm is stable.

Ca^{2+} handling system stability

The results in Fig. 2 demonstrate the effect of changing the morphology of the action potential waveform during voltage clamping at a single pacing period. Fig. 3 explores the effect of changing the morphology of the action potential on the stability of the Ca^{2+} handling system over a range of values of *T*. Simulations using three values of β (0.9, 1.5, and 2.0) are shown, with the bifurcation diagrams in Fig. 3 *A* depicting the peak value of $[Ca^{2+}]_i$ from two consecutive beats at steady state plotted as a function of *T*. The variety of β values reflects different combinations of ionic conductances that generate a range of action potential morphologies.

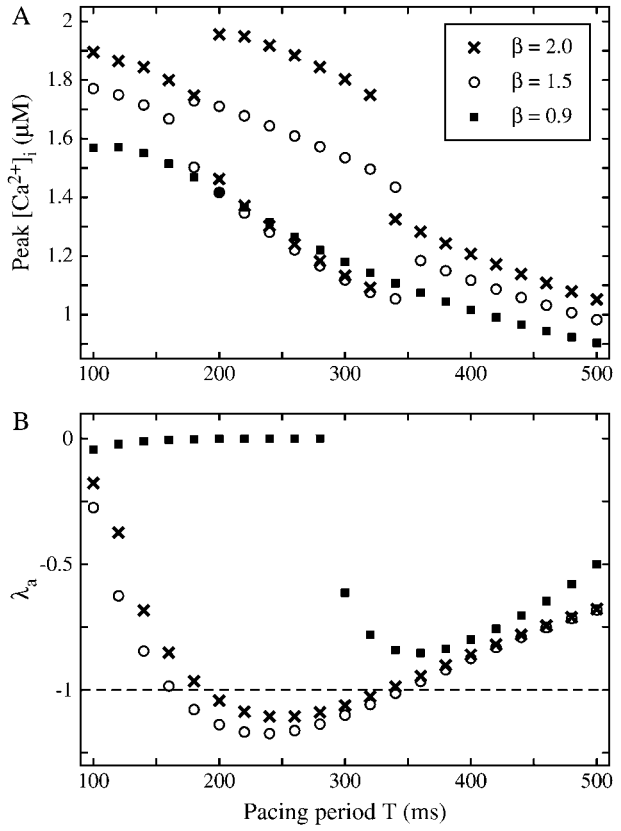

FIGURE 3 (*A*) Bifurcation diagrams illustrating peak $[Ca^{2+}]_i$ from two consecutive beats as a function of pacing period for the three values of β shown in Fig. 1. Ca^{2+} alternans occurs over a range of pacing periods for $\beta = 2.0$ and $\beta = 1.5$, but alternans is absent at all pacing periods for $\beta = 0.9$. (*B*) Alternans eigenvalue (λ_a) as a function of pacing period for the same values of β and *T* as in panel *A*. As panel *B* shows, λ_a for each value of β and *T* in panel *A* indicates the presence or absence of alternans, with the presence of alternans characterized by $|\lambda_a|>1$ and the absence of alternans characterized by $|\lambda_a|<1$.

Fig. 3 *A* shows that, for $\beta = 1.5$ and $\beta = 2.0$, peak $[Ca^{2+}]_i$ alternates over a range of pacing periods. For $\beta = 2.0$, alternans occurs between $T = 320$ ms and $T = 200$ ms, whereas for $\beta = 1.5$ alternans occurs between $T = 340$ ms and $T = 180$ ms. In contrast, there is no alternans for $\beta = 0.9$ at any value of T. This indicates that how the action potential morphology changes as a function of the pacing period is important in determining whether Ca^{2+} alternans will occur at any given value of T.

Fig. 3 *B* illustrates the alternans eigenvalue (λ_a) calculated for the same values of β and T as in Fig. 3 *A*. Fig. 3 *B* shows that $|\lambda_a|>1$ for every set of conditions (i.e., each combination of β and T) where Ca^{2+} alternans occurs in Fig. 3 *A*, whereas $|\lambda_a|<1$ corresponds to the stable period-1 behavior seen in Fig. 3 *A*. Although $|\lambda_a|$ indicates the absence or presence of alternans (i.e., the degree of stability of the system), Fig. 3 also shows that there is no correlation between $|\lambda_a|$ and the magnitude of alternans (measured as the difference between the peak $[Ca^{2+}]_i$ from two consecutive beats in Fig. 3 *A*). For example, the period-1 solution for $\beta = 1.5$ becomes more unstable than the period-1 solution for $\beta = 2.0$ (indicated by the larger $|\lambda_a|$ in Fig. 3 *B*), but the magnitude of alternans is always smaller for $\beta = 1.5$ than for $\beta = 2.0$. Therefore, alternans magnitude cannot be used as a measure of the degree of instability of the system.

Transition to Ca^{2+} alternans

As Fig. 3 *B* indicates, the nonalternating period-1 behavior becomes very stable (i.e., $|\lambda_a| \ll 1$) for action potential waveforms corresponding to $\beta = 0.9$ at pacing periods shorter than $T = 300$ ms. This is in stark contrast to the situation for $\beta = 1.5$, where the period-1 solution is unstable between $T = 340$ ms and $T = 180$ ms. At each pacing period over this range, the nonalternating period-1 solution becomes unstable at some value of β between 0.9 and 1.5. To explore the transition to instability, the value of β was varied at three different values of T, and λ_a for each value of β and T was calculated. The resulting values of λ_a, shown in Fig. 4 *A*, are plotted as a function of the action potential duration at 50% repolarization (APD_{50}). For reference, the relationships between APD_{50} and β for each value of T are illustrated in Fig. 4 *B*.

As Fig. 4 *A* illustrates, the stability of the nonalternating period-1 solution is highly sensitive to the morphology of the action potential (as measured by APD_{50}) at each pacing period, with the transition to instability resulting from small changes in APD_{50} when $T = 250$ ms and $T = 320$ ms. For both of these values of T, the nonalternating period-1 rhythm reaches a maximal level of instability as APD_{50} is lengthened, and in both cases the period-1 rhythm remains unstable until the last data point shown. At $T = 400$ ms, changing the morphology of the action potential is not sufficient to force the system to cross the stability boundary ($|\lambda_a| = 1$). However, the system does become markedly less stable as the action potential morphology changes, with this reduction in stability similarly occurring in response to a very small change in morphology.

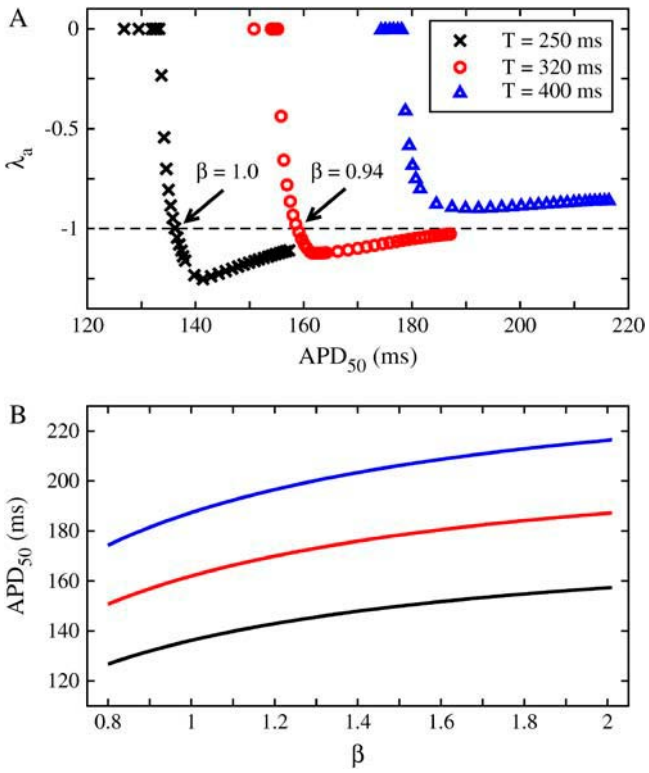

FIGURE 4 (*A*) Alternans eigenvalue (λ_a) as a function of APD_{50} at pacing periods $T = 250$ ms (*black crosses*), $T = 320$ ms (*red circles*), and $T = 400$ ms (*blue triangles*). For $T = 250$ ms and $T = 320$ ms, the transition from no alternans to alternans is characterized by a rapid change in λ_a, with the switch from a very stable Ca^{2+} handling system to an unstable system occurring in response to a very small change in action potential morphology (as measured by the action potential duration at 50% repolarization [APD_{50}]). For $T = 400$ ms, the period-1 solution becomes much less stable in response to changes in action potential morphology, but does not become unstable. (*B*) The relationships between β and APD_{50} for $T = 250$ ms (*black line*), $T = 320$ ms (*red line*), and $T = 400$ ms (*blue line*).

Stability sensitivity

Fig. 5 illustrates, for two action potential morphologies (corresponding to $\beta = 1.0$ and $\beta = 2.0$) and pacing periods ($T = 250$ ms and $T = 333$ ms, respectively), the sensitivity of λ_a to changes in the contribution of particular components of the Ca^{2+} handling system (changes that mimic, for example, the effects of pharmacological agents). Two of the components (u, v_{up}) are related to the sarcoplasmic reticulum, and two (g_{Ca}, g_{NaCa}) are related to the sarcolemmal Ca^{2+} currents. At baseline (corresponding to the 0% line) in both cases, $\lambda_a \approx -1$, indicating that the system is sitting on the stability boundary.

Fig. 5 suggests that: i), changing any parameter in the model affects the stability of the Ca^{2+} handling system (i.e.,

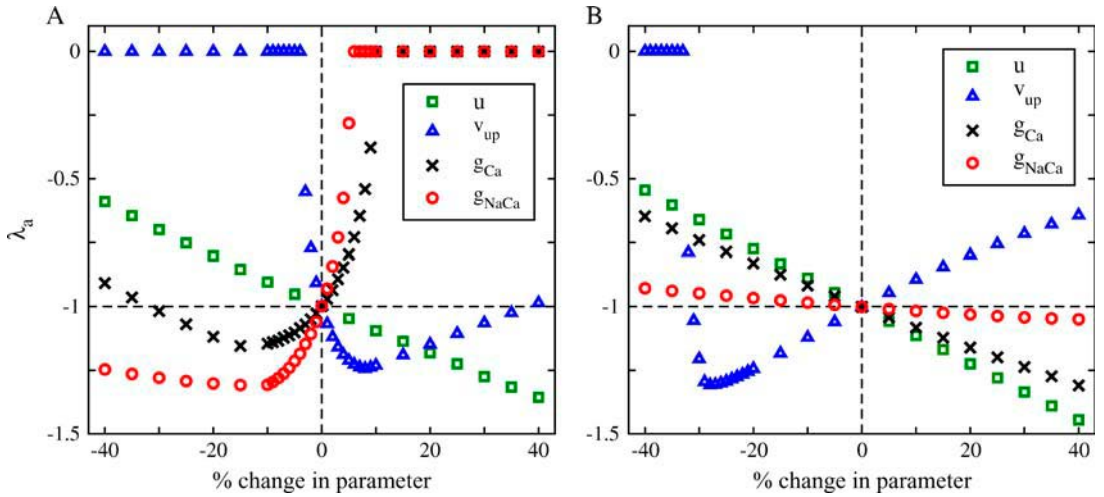

FIGURE 5 Sensitivity of the transition to Ca^{2+} alternans to changes in the contribution of various components of the Ca^{2+} handling system. (*A*) $\beta = 1.0$, $T = 250$ ms; (*B*) $\beta = 2.0$, $T = 333$ ms. At baseline (i.e., 0% change) in both cases, the system is sitting on the stability boundary (i.e., $|\lambda_a| = 1$). Increasing or decreasing the contribution of any part of the Ca^{2+} handling system (i.e., moving to the left or the right along the axis) changes the stability of the entire system. u = slope of the sarcoplasmic reticulum (*SR*) Ca^{2+} release function; v_{up} = *SR* uptake pump strength; g_{Ca} = maximum conductance of the L-type Ca^{2+} channels; g_{NaCa} = Na^{+}-Ca^{2+} exchanger strength.

changes the value of λ_a) in the neighborhood of the transition from no alternans to alternans (i.e., in the neighborhood of the transition to the unstable period-1 solution); ii), the degree of sensitivity of the stability of the Ca^{2+} handling system is parameter dependent; and iii), particular parameter changes can have qualitatively different stability effects for different baseline states (e.g., increasing g_{Ca} or g_{NaCa} from baseline causes an increase in stability when $\beta = 1.0$, but a decrease in stability when $\beta = 2.0$).

Fig. 6 further explores the sensitivity of the system by systematically changing the four components studied in Fig. 5 while also varying the pacing period and action potential morphology. Fig. 6 illustrates the influence of increasing and decreasing by 20% the maximum conductance of the L-type Ca^{2+} channels (Fig. 6 *A*), the Na^{+}-Ca^{2+} exchanger strength (Fig. 6 *B*), the SR uptake pump strength (Fig. 6 *C*), and the slope of the SR Ca^{2+} release function (Fig. 6 *D*) on the alternans eigenvalue over a range of pacing periods when $\beta = 0.9$ and $\beta = 2.0$. In both cases, the eigenvalues at baseline (i.e., 0% change) are identical to those shown in Fig. 3 *B*.

Fig. 6 reveals that when the action potential morphology is changed, the same percentage change in the contribution of a component of the Ca^{2+} handling system can have markedly different effects on the stability of the system as a function of pacing period. When $\beta = 2.0$, 20% changes in each of the four parameters in either direction result in fairly small changes to the stability of the system. However, when $\beta = 0.9$, the same Ca^{2+} handling system subjected to the same 20% changes but a different action potential morphology results in markedly different stability properties. For example, a reduction of the Na^{+}-Ca^{2+} exchanger strength (Fig. 6 *B*) by 20% causes a very slight stabilization of the Ca^{2+} handling system compared to baseline for all pacing periods when $\beta = 2.0$. However, the same 20% reduction in I_{NaCa} for action potentials whose morphology is characterized by $\beta = 0.9$ destabilizes the system compared to baseline, with the amount of destabilization (as measured by the distance between the 0 and -20% alternans eigenvalues) varying widely as a function of pacing period.

Restitution curve slope

Fig. 3 indicates that how action potential morphology changes as a function of the pacing period is important in determining whether alternans will occur at a given value of T. To determine whether a relationship exists between the occurrence of Ca^{2+} alternans and the slope of the APD restitution curve, the slopes of the APD restitution curves characterizing the action potentials imposed during voltage clamping were calculated, and these slopes were plotted as a function of DI as shown in Fig. 7 *A*. The slopes of the restitution curves at 50% repolarization were used, because (as Fig. 1 *B* shows) the restitution curves at 90% repolarization for the three values of β used in Fig. 1 are identical. Fig. 7 *B* illustrates the alternans eigenvalues from Fig. 3 *B* at the same values of β as in Fig. 7 *A*, also plotted as a function of DI.

Fig. 7 shows that, for $\beta = 2.0$ and $\beta = 1.5$, Ca^{2+} alternans occurs under conditions corresponding to the APD restitution curve slope being at times <1 and at times >1. For $\beta = 0.9$, however, Ca^{2+} alternans is absent for all values of DI (as Fig. 7 *B* indicates), even for values of DI corresponding to a slope of the APD restitution curve >1. These results indicate that there is no correlation between the slope of the APD_{50} restitution curve and the occurrence of Ca^{2+} alternans. Although not shown, no correlation was found

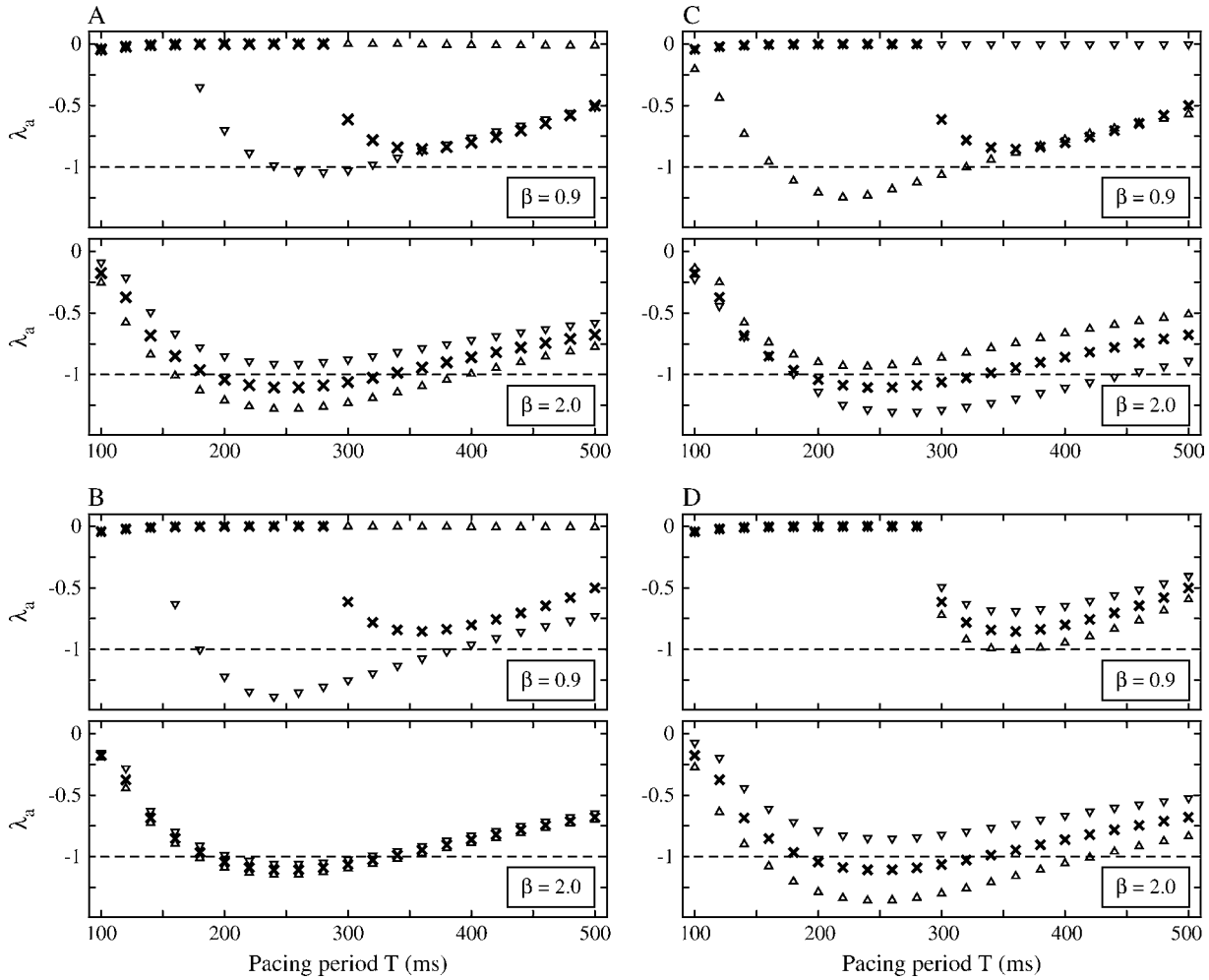

FIGURE 6 Sensitivity of λ_a to +20% (△) and −20% (∇) changes in the contribution of (*A*) maximum conductance of the L-type Ca^{2+} channels (g_{Ca}), (*B*) the Na^+-Ca^{2+} exchanger strength (g_{NaCa}), (*C*) the SR uptake pump strength (v_{up}), and (*D*) the slope of the sarcoplasmic reticulum Ca^{2+} release function (u) for $\beta = 0.9$ (*top panels*) and $\beta = 2.0$ (*bottom panels*). Crosses indicate λ_a at baseline (identical to Fig. 3 *B*).

between the slopes of the APD_{90} restitution curves and the presence of Ca^{2+} alternans.

DISCUSSION

The results of this study indicate that, at any given excitation rate, the stability of the intracellular Ca^{2+} handling system is intimately linked to the temporal dynamics of membrane voltage. By changing the morphology of the action potential at a given excitation rate, qualitatively different behaviors of the Ca^{2+} handling system (either nonalternating or alternating Ca^{2+} transients) can be induced.

Whole-cell dependence of Ca^{2+} handling

The Ca^{2+} handling system in healthy cardiac myocytes possesses the ability to exquisitely control $[Ca^{2+}]_i$ (28). Normally, the amount of Ca^{2+} that enters a myocyte during each beat is exactly equal to the amount of Ca^{2+} that is pumped out, and the amount of Ca^{2+} that is released by the SR during each beat is equal to the amount that is returned to the SR (28). If a single beat provides insufficient time to allow this Ca^{2+} cycling process to reach steady state (as may occur at rapid excitation rates), the Ca^{2+} cycling process may instead reach steady state after every second beat. This will be manifested as an alternation in the shape of the Ca^{2+} transient on a beat-to-beat basis.

Certain elements of the Ca^{2+} handling system appear to be important in determining the conditions under which Ca^{2+} alternans occurs. Particular emphasis has recently been placed on the characteristics of the SR (32), with this emphasis stemming from insights both from experimental work (13) and from mathematical modeling (19,28,29). In this study we have instead focused on the influence of membrane voltage on the behavior of the Ca^{2+} handling system. We found that membrane voltage, which affects the system through the sarcolemmal currents I_{Ca} and I_{NaCa}, plays an important role in determining when Ca^{2+} alternans occurs.

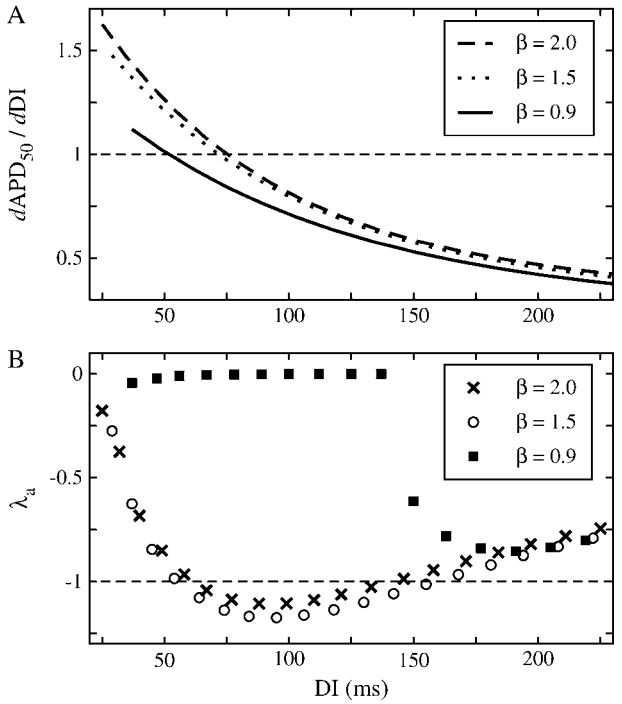

FIGURE 7 (*A*) Slopes of the restitution curves from Fig. 1 *B* (50% repolarization). (*B*) λ_a for the same values of β as shown in panel *A*, plotted as a function of diastolic interval.

Our results suggest that the conditions under which Ca^{2+} alternans occurs are governed not by any one part of the Ca^{2+} handling system, but by the entire interconnected system. From a dynamical systems perspective, this result is not surprising. The highly interconnected nature of the Ca^{2+} handling system means that every component must be considered when attempting to understand the stability properties of the system in the neighborhood of the transition from a stable to unstable period-1 solution. It is not sufficient to draw conclusions about the stability properties of the entire system by studying each component of the system in isolation, as this does not allow for the compensatory effects of other components. For this reason, techniques such as the ''eigenmode'' method are crucial for understanding complex physiological processes in their entirety (10). By taking into account every component of the model Ca^{2+} handling system with this method, we are able to analyze the stability properties of the system in the neighborhood of the transition to alternans, and thereby predict the occurrence of Ca^{2+} alternans.

Slope of the restitution curve

Several studies have suggested a relationship between the slope of the APD restitution curve and the occurrence of electrical alternans (33–39). These studies are based on the restitution hypothesis, which states that electrical alternans will occur when the slope of the APD restitution curve is >1. We sought to determine whether a relationship exists between the slope of the APD restitution curve during action potential voltage clamping and the occurrence of Ca^{2+} alternans.

As Fig. 7 indicates, there is no simple relationship between the slope of the APD restitution curve and the occurrence of Ca^{2+} alternans in this model. Even though the slopes of the three restitution curves shown in Fig. 1 all became >1 at short DIs, Ca^{2+} alternans did not uniformly occur for all action potential morphologies when the slopes of the respective APD restitution curves were >1. This finding is consistent with a number of recent studies that have found that the slope of the APD restitution curve is not an accurate predictor of the conditions under which alternans occurs (10,12,16,40, 41). As our results indicate, the only accurate predictor of whether Ca^{2+} alternans will occur is the alternans eigenvalue.

Membrane currents and Ca^{2+} handling

During action potential voltage clamping, the predominant membrane currents influencing the dynamics of the Ca^{2+} handling system are Ca^{2+} currents (such as I_{Ca} and I_{NaCa} in the model used here). During unclamped action potentials, however, every membrane current in the myocyte contributes to shaping the membrane voltage as a function of time, and thus every membrane current contributes to the voltage that is sensed by the Ca^{2+}-selective currents. Given that our results suggest that the morphology of the action potential plays a key role in determining the stability of the Ca^{2+} handling system, it follows that every membrane current in the myocyte (through its influence on membrane voltage) plays a role in modulating the stability of the Ca^{2+} handling system.

This has important implications for electrical alternans. If the hypothesis that intracellular Ca^{2+} alternans leads to electrical alternans is correct (26), the unclamped action potential would be expected to alternate when the Ca^{2+}-selective currents such as I_{Ca} and I_{NaCa} begin to alternate. Therefore, a change in the contribution of any membrane current when the action potential is not clamped should alter the stability of the Ca^{2+} handling system and, in turn, should change the conditions under which Ca^{2+} alternans and, therefore, electrical alternans, occurs. This prediction is borne out in Fig. 8.

Fig. 8 was generated using a complete ionic model of the myocyte that incorporates the Ca^{2+} handling system used in this study (19). Instead of being clamped by a predetermined waveform, the membrane voltage in the complete ionic model varies dynamically in response to the contribution of a number of membrane currents including I_{Na}, I_{Kr}, I_{Ks}, I_{to}, and I_{K1}. During action potential voltage clamping, the Ca^{2+} handling system of the complete ionic model exhibits alternans (just as the action potential clamp model used elsewhere in this study does). When membrane voltage is not clamped,

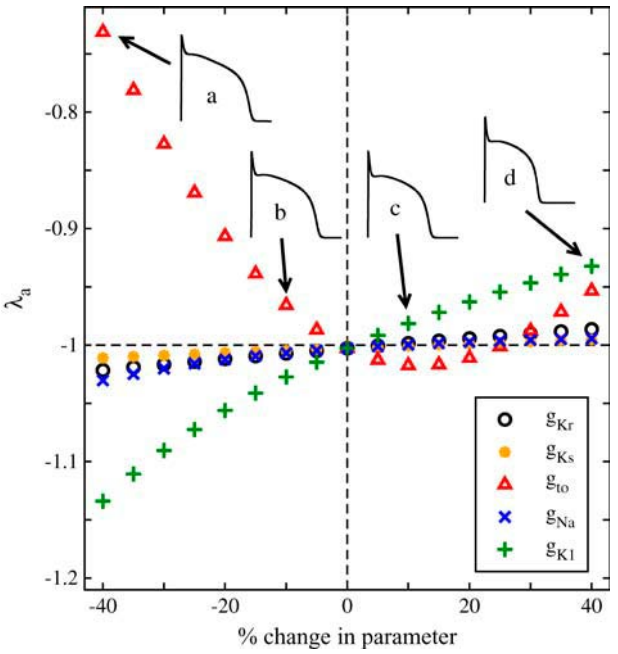

FIGURE 8 Stability of the complete ionic model of the ventricular action potential, incorporating the Ca^{2+} handling system used in Figs. 1–7. Action potentials in the model were elicited by brief suprathreshold current injections at a pacing period of 365 ms. A change in the contribution of any of the membrane currents shown causes the morphology of the action potential to change (see *insets a–d*; APD_{50} for $a = 194$ ms, $b = 185$ ms, $c = 172$ ms, $d = 151$ ms), which causes the stability of the system to change as well (as reflected in λ_a). In some cases, the system becomes more stable, and in other cases the system moves into the unstable regime. It should be noted that action potentials *a–d* demonstrate that stability is not simply a function of APD, as the longer (*a*) and shorter (*d*) action potentials are more stable than the intermediate (*b* and *c*) action potentials. It is also worth noting that the stabilization seen as g_{Kr} increases is consistent with previous experimental findings demonstrating that increased I_{Kr} expression can suppress alternans (15). In the complete ionic model, $u = 11.3$ (same as for the voltage clamp model), $\gamma = 0.7$, and $\tau_f = 30$ ms. g_{Kr} = maximum conductance of the fast component of the delayed rectifier potassium current; g_{Ks} = maximum conductance of the slow component of the delayed rectifier potassium current; g_{to} = maximum conductance of the transient outward potassium current; g_{Na} = maximum conductance of the fast sodium current; g_{K1} = maximum conductance of the inward rectifier potassium current.

however, all components of the model alternate simultaneously, and λ_a becomes a measure of the stability of the complete interconnected system. In Fig. 8, the stability of the entire system, including the contribution of membrane currents, is shown.

The simulations in Fig. 8 are very similar to those in Fig. 3, where the morphology of the action potential during voltage clamping was changed directly and the effect on the stability of the system was determined. In Fig. 8, however, the morphology of the action potential is changed indirectly by varying the conductances of five sodium and potassium currents (to mimic, for example, the effects of pharmacological agents, or the effects of altered channel protein expression (15)). At baseline (i.e., at 0%), $\lambda_a \approx -1$, indicating that the system is sitting on the stability boundary. As predicted, changing the contribution of any membrane current at a given pacing period changes the stability characteristics of the system, and thereby changes the conditions under which Ca^{2+} alternans (and, therefore, electrical alternans) occurs. This suggests that every membrane current contributes to the stability of the Ca^{2+} handling system in the neighborhood of the transition from a stable to unstable period-1 solution and, hence, every membrane current contributes to establishing the conditions under which electrical alternans occurs.

Limitations

The results in this study were obtained using a mathematical model of the rabbit ventricular myocyte intracellular Ca^{2+} handling system. Although it is likely that there are quantitative differences between the model system and the human ventricular myocyte Ca^{2+} handling system, we expect the basic finding of this work—that the stability of the Ca^{2+} handling system is modulated by the morphology of the action potential and, therefore, by all membrane currents—to be valid. Although our results were obtained from simulated cardiac myocytes, this finding can, in principle, be tested experimentally.

This research was supported by a Whitaker Foundation Biomedical Engineering Research Grant (No. RG-02-0369). Peter Jordan was also supported by a Predoctoral Fellowship from the Howard Hughes Medical Institute.

REFERENCES

1. Adam, D. R., J. M. Smith, S. Akselrod, S. Nyberg, A. O. Powell, and R. J. Cohen. 1984. Fluctuations in T-wave morphology and susceptibility to ventricular fibrillation. *J. Electrocardiol.* 17:209–218.
2. Smith, J. M., E. A. Clancy, C. R. Valeri, J. N. Ruskin, and R. J. Cohen. 1988. Electrical alternans and cardiac electrical instability. *Circulation.* 77:110–121.
3. Nearing, B. D., A. H. Huang, and R. L. Verrier. 1991. Dynamic tracking of cardiac vulnerability by complex demodulation of the T wave. *Science.* 252:437–440.
4. Rosenbaum, D. S., L. E. Jackson, J. M. Smith, H. Garan, J. N. Ruskin, and R. J. Cohen. 1994. Electrical alternans and vulnerability to ventricular arrhythmias. *N. Engl. J. Med.* 330:235–241.
5. Tachibana, H., I. Kubota, M. Yamaki, T. Watanabe, and H. Tomoike. 1998. Discordant S-T alternans contributes to formation of reentry: a possible mechanism of reperfusion arrhythmia. *Am. J. Physiol.* 275:H116–H121.
6. Pastore, J. M., S. D. Girouard, K. R. Laurita, F. G. Akar, and D. S. Rosenbaum. 1999. Mechanism linking T-wave alternans to the genesis of cardiac fibrillation. *Circulation.* 99:1385–1394.
7. Qu, Z., A. Garfinkel, P. S. Chen, and J. N. Weiss. 2000. Mechanisms of discordant alternans and induction of reentry in simulated cardiac tissue. *Circulation.* 102:1664–1670.
8. Watanabe, M. A., F. H. Fenton, S. J. Evans, H. M. Hastings, and A. Karma. 2001. Mechanisms for discordant alternans. *J. Cardiovasc. Electrophysiol.* 12:196–206.
9. Walker, M. L., X. Wan, G. E. Kirsch, and D. S. Rosenbaum. 2003. Hysteresis effect implicates calcium cycling as a mechanism of repolarization alternans. *Circulation.* 108:2704–2709.

10. Li, M., and N. F. Otani. 2003. Ion channel basis for alternans and memory in cardiac myocytes. *Ann. Biomed. Eng.* 31:1213–1230.

11. Laurita, K. R., R. Katra, B. Wible, X. Wan, and M. H. Koo. 2003. Transmural heterogeneity of calcium handling in canine. *Circ. Res.* 92: 668–675.

12. Cherry, E. M., and F. H. Fenton. 2004. Suppression of alternans and conduction blocks despite steep APD restitution: electrotonic, memory, and conduction velocity restitution effects. *Am. J. Physiol.* 286:H2332–H2341.

13. Diaz, M. E., S. C. O'Neill, and D. A. Eisner. 2004. Sarcoplasmic reticulum calcium content fluctuation is the key to cardiac alternans. *Circ. Res.* 94:650–656.

14. Sipido, K. R. 2004. Understanding cardiac alternans: the answer lies in the Ca^{2+} store. *Circ. Res.* 94:570–572.

15. Hua, F., D. C. Johns, and R. F. Gilmour, Jr. 2004. Suppression of electrical alternans by overexpression of HERG in canine ventricular myocytes. *Am. J. Physiol.* 286:H2342–H2351.

16. Pruvot, E. J., R. P. Katra, D. S. Rosenbaum, and K. R. Laurita. 2004. Role of calcium cycling versus restitution in the mechanism of repolarization alternans. *Circ. Res.* 94:1083–1090.

17. Goldhaber, J. I., L. H. Xie, T. Duong, C. Motter, K. Khuu, and J. N. Weiss. 2005. Action potential duration restitution and alternans in rabbit ventricular myocytes: the key role of intracellular calcium cycling. *Circ. Res.* 96:459–466.

18. Lakireddy, V., P. Baweja, A. Syed, G. Bub, M. Boutjdir, and N. El-Sherif. 2005. Contrasting effects of ischemia on the kinetics of membrane voltage and intracellular calcium transient underlie electrical alternans. *Am. J. Physiol.* 288:H400–H407.

19. Shiferaw, Y., D. Sato, and A. Karma. 2005. Coupled dynamics of voltage and calcium in paced cardiac cells. *Phys Rev E.* 71:021903.

20. Rappel, W. J., F. Fenton, and A. Karma. 1999. Spatiotemporal control of wave instabilities in cardiac tissue. *Phys. Rev. Lett.* 83:456–459.

21. Hall, G. M., and D. J. Gauthier. 2002. Experimental control of cardiac muscle alternans. *Phys. Rev. Lett.* 88:198102.

22. Echebarria, B., and A. Karma. 2002. Spatiotemporal control of cardiac alternans. *Chaos.* 12:923–930.

23. Allexandre, D., and N. F. Otani. 2004. Preventing alternans-induced spiral wave breakup in cardiac tissue: an ion-channel-based approach. *Phys Rev E.* 70:061903.

24. Li, M., and N. F. Otani. 2004. Controlling alternans in cardiac cells. *Ann. Biomed. Eng.* 32:784–792.

25. Jordan, P. N., and D. J. Christini. 2004. Adaptive diastolic interval control of cardiac action potential duration alternans. *J. Cardiovasc. Electrophysiol.* 15:1177–1185.

26. Walker, M. L., and D. S. Rosenbaum. 2003. Repolarization alternans: implications for the mechanism and prevention of sudden cardiac death. *Cardiovasc. Res.* 57:599–614.

27. Chudin, E., J. Goldhaber, A. Garfinkel, J. Weiss, and B. Kogan. 1999. Intracellular Ca^{2+} dynamics and the stability of ventricular tachycardia. *Biophys. J.* 77:2930–2941.

28. Eisner, D. A., H. S. Choi, M. E. Diaz, S. C. O'Neill, and A. W. Trafford. 2000. Integrative analysis of calcium cycling in cardiac muscle. *Circ. Res.* 87:1087–1094.

29. Shiferaw, Y., M. A. Watanabe, A. Garfinkel, J. N. Weiss, and A. Karma. 2003. Model of intracellular calcium cycling in ventricular myocytes. *Biophys. J.* 85:3666–3686.

30. Wan, X., K. R. Laurita, E. J. Pruvot, and D. S. Rosenbaum. 2005. Molecular correlates of repolarization alternans in cardiac myocytes. *J. Mol. Cell. Cardiol.* 39:419–428.

31. Sah, R., R. J. Ramirez, and P. H. Backx. 2002. Modulation of Ca^{2+} release in cardiac myocytes by changes in repolarization rate: role of phase-1 action potential repolarization in excitation-contraction coupling. *Circ. Res.* 90:165–173.

32. Eisner, D. A., M. E. Diaz, Y. Li, C. O'Neill, and A. W. Trafford. 2005. Stability and instability of regulation of intracellular calcium. *Exp. Physiol.* 90:3–12.

33. Nolasco, J. B., and R. W. Dahlen. 1968. A graphic method for the study of alternation in cardiac action potentials. *J. Appl. Physiol.* 25:191–196.

34. Guevara, M. R., G. Ward, A. Shrier, and L. Glass. 1984. Electrical alternans and period-doubling bifurcations. *Comput. Cardiol.* 11:167–170.

35. Karma, A. 1994. Electrical alternans and spiral wave breakup in cardiac tissue. *Chaos.* 4:461–472.

36. Koller, M. L., M. L. Riccio, and R. F. Gilmour, Jr. 1998. Dynamic restitution of action potential duration during electrical alternans and ventricular fibrillation. *Am. J. Physiol.* 275:H1635–H1642.

37. Tolkacheva, E. G., D. G. Schaeffer, D. J. Gauthier, and W. Krassowska. 2003. Condition for alternans and stability of the 1:1 response pattern in a ''memory'' model of paced cardiac dynamics. *Phys Rev E.* 67:031904.

38. Tolkacheva, E. G., M. M. Romeo, M. Guerraty, and D. J. Gauthier. 2004. Condition for alternans and its control in a two-dimensional mapping model of paced cardiac dynamics. *Phys Rev E.* 69:031904.

39. Kalb, S. S., H. M. Dobrovolny, E. G. Tolkacheva, S. F. Idriss, W. Krassowska, and D. J. Gauthier. 2004. The restitution portrait: a new method for investigating rate-dependent restitution. *J. Cardiovasc. Electrophysiol.* 15:698–709.

40. Banville, I., and R. A. Gray. 2002. Effect of action potential duration and conduction velocity restitution and their spatial dispersion on alternans and the stability of arrhythmias. *J. Cardiovasc. Electrophysiol.* 13:1141–1149.

41. Fox, J. J., E. Bodenschatz, and R. F. Gilmour, Jr. 2002. Period-doubling instability and memory in cardiac tissue. *Phys. Rev. Lett.* 89: 138101.